Natural Hazards (2005) 35: 185–209
DOI 10.1007/s11069-004-4809-3

Estimation of Tsunami Risk for the Coasts of Peru and Northern Chile

EVGUENI A. KULIKOV[1,2], ALEXANDER B. RABINOVICH[1,2] and RICHARD E. THOMSON[1]
[1]*Department of Fisheries and Oceans, Institute of Ocean Sciences, 9860 West Saanich Rd., Sidney, BC, Canada V8L 4B2 (E-mails: KulikovE@pac.dfo-mpo.gc.ca; RabinovichA@pac.dfo-mpo.gc.ca; ThomsonR@pac.dfo-mpo.gc.ca);* [2]*P.P. Shirshov Institute of Oceanology, Russian Academy of Sciences 36 Nakhimovsky Prosp., Moscow, 117997, Russia (E-mail: kulikov@korolev.net.ru, abr@iki.rssi.ru)*

(Received: 18 February 2004; accepted: 10 October 2004)

Abstract. Data for tsunamigenic earthquakes and observed tsunami run-up are used to estimate tsunami-risk for the coasts of Peru and northern Chile for zones bounded by 5–35° S latitude. Tsunamigenic earthquake estimates yield magnitudes of 8.52, 8.64, and 8.73 for recurrence periods of 50, 100, and 200 years, respectively. Based on three different empirical relations between earthquake magnitudes and tsunamis, we estimate expected tsunami wave heights for various return periods. The average heights were 11.2 m (50 years), 13.7 m (100 years), and 15.9 m (200 years), while the maximum height values (obtained by Iida's method) were: 13.9, 17.3, and 20.4 m, respectively. Both the "averaged" and "maximum" seismological estimates of tsunami wave heights for this region are significantly smaller than the actually observed tsunami run-up of 24–28 m, for the major events of 1586, 1724, 1746, 1835, and 1877. Based directly on tsunami run-up data, we estimate tsunami wave heights of 13 m for a 50-year return period and 25 m for a 100-year return period. According to the "seismic gap" theory, we can expect that the next strong earthquake and tsunami will occur between 19 and 28° S in the vicinity of northern Chile.

Key words: tsunami risk, tsunami wave height, return period, Peru, Chile, earthquake, seismic gap theory

1. Introduction

Tsunamis are among the world's most destructive natural hazards. To mitigate the loss of life and property, the possible impact of tsunami waves must be taken into account prior to major development or construction in seismically active regions of the ocean coast. The recent 12 years (1992–2003) have been characterized by anomalously high tsunami activity in the World Ocean. More than 20 catastrophic tsunamis occurred during this period, including the February 21, 1996 tsunami off Chimbote, northern Peru, the July 17, 1998 tsunami in Papua New Guinea, and the June 23, 2001 tsunami off the Camaná–Chala region, Southern Peru. These tsunamis were responsible for extensive property damage and about 4,000 deaths. The devastating Papua New Guinea tsunami killed about 2,200 villagers, including more than 230 children (González, 1999). Surprisingly, the large waves associated with the Papua New Guinea tsunami were generated by a relatively small earthquake ($M_w = 7.1$), indicating that destructive tsunami waves are not confined to earthquakes with extreme magnitudes.

The 1996 Chimbote tsunami was associated with a $M_w = 7.5$ offshore subduction-zone earthquake off northern Peru. A total of 12 people were killed and 57 injured by the tsunami (Heinrich *et al.*, 1998). This tsunami was the first in Peru's history to be subjected to an extensive post-tsunami field survey (Bourgeois *et al.*, 1999). The greatest tsunami runup (5.14 m) was found on the north side of Chimbote Bay.

The June 23, 2001 tsunami was initiated by a major ($M_w = 8.4$) earthquake off the coast of southern Peru. According to the Peruvian government, approximately 80 people were killed and 70 people were missing. A total of 200,000 people were affected by the earthquake (Rodriguez-Marek and Edwards, 2003). This earthquake also generated a widespread tsunami, which claimed at least 23 additional lives and was recorded at many sites along the Pacific coast, including New Zealand (Goring, 2002) and Canada (Rabinovich and Stephenson, 2004). Rabinovich *et al.*, (2001) had predicted such a catastrophic earthquake and tsunami for this region of Peru.

Long-term tsunami prediction (*tsunami-zoning*) is of key importance for tsunami research and coastal engineering problems, especially for areas of new construction. Creation of complex and/or expensive structures in coastal areas requires reliable estimation of extreme tsunami run-up and run-down. Overestimation of the tsunami risk significantly increases the cost of construction, whereas underestimation of possible tsunami heights may have catastrophic consequences, including widespread destruction of property and loss of life. Tsunami-zoning involves the estimation of maximum tsunami heights, the corresponding inundation (or draw down), and the recurrence times for major tsunami events (cf. Planning for Risk, 1988; Rabinovich *et al.*, 1992; Mofjeld *et al.*, 1999).

The purpose of this study is to provide estimates of tsunami wave heights and possible run-up for the coastal area of southern Peru and northern Chile. This coast has an extensive recorded history of tsunamigenic earthquakes dating back to the beginning of the 16th century and remains one of the most seismically active regions in the world. A difficulty with studying tsunamis in this area is a lack of tsunami data, especially for the border region between Peru and Chile. This lack of information is exacerbated by the fact that resonant features of the local topography may significantly affect tsunami waves approaching the coast, resulting in strong spatial variations of tsunami wave heights. Detailed numerical modeling of tsunami waves, combined with observational data (where such data are available) is a common approach for local tsunami zoning (cf. Khramushin and Shevchenko, 1994; Mofjeld *et al.*, 1999). Because the present study is limited by the fragmentary nature of the historical data, we present only preliminary estimates of possible tsunami wave heights. Moreover, these estimates are related to the entire examined coast and not to a specific site. More precise estimates for particular areas can only be obtained through detailed numerical modeling of regional tsunami waves that takes into account resonant features of the regional and local seafloor topography and coastline.

An abridged version of this study was presented by Rabinovich *et al.* (2001) at the Tsunami Symposium in Seattle in 2001. Additional information and historical data obtained since the time of the symposium, together with the data from the recent Peru tsunami of June 23, 2001, allowed us to complete this study and to verify the previous estimates.

2. Historical Tsunami Data

The first recorded observations of earthquakes and tsunamis for the Pacific coast of South America date back to the 16th century when Spain established its rule over the New World. Additional descriptions of ancient catastrophic events (earthquakes and sea floods) may be found in Peruvian and Chilean legends (Soloviev and Go, 1975). In particular, ancient Indian chronicles tell us that Peru had several strong earthquakes "causing high mountains to collapse" during which time the ocean showed "significant oscillations". The first scientific examination of earthquakes and tsunamis for the Pacific coast of South America began in 20th century with Berninghausen (1962) who listed 49 tsunamis from 1562 to 1960, from which 23 tsunamis probably impacted the area of study. Further examination of South American tsunamis has been undertaken by Lomnitz (1970), Soloviev and Go (1975), and Lockridge (1985). According to the map of tsunamigenic earthquakes for the period 1562–1960 constructed by Soloviev and Go (1975), almost the entire coast of South America is a zone of high tsunami hazard.

A difficulty with studying tsunamis in the region of southern Peru and northern Chile is that it is located far from the capitals of either country. As with most nations, Chilean and Peruvian chronicles focus most their attention on more heavily populated regions of the respective countries, in this case the areas of Santiago, Valparaiso, and Concepcion (Chile) and Lima, Callao, and Pisco (Peru). The problem is compounded by a lack of tide gauge data; the only tide gauges near the Peru/Chile border are Arica (Chile) and Matarani (Peru).

Our search of the catalogues focuses on all available information for the region of Peru and northern Chile. Based on historical tsunami data, we identify four types of tsunamis capable of impacting the study region:

(1) Trans-Pacific tsunamis;
(2) Regional tsunamis;
(3) Local tsunamis;
(4) Landslide-generated tsunamis.

Trans-Pacific tsunamis are tsunamis generated by major earthquakes whose epicenters are located along the Pacific Rim, encompassing areas of Alaska, the Aleutian Islands, the Kamchatka Peninsula, the Kuril Islands, Japan, the Philippines, and Indonesia. Trans-Pacific tsunamis were reported this century for the coasts of Peru and Chile in 1946, 1952, 1957, 1960, 1964, 1968, 1975, and 1994. Maximum observed wave heights were 3–4 m (Lockridge, 1985). However, the probability of a catastrophic trans-Pacific tsunami with wave heights exceeding several meters for the Peruvian and Chilean coast is low. Ships docked at the docking facility are expected to receive the needed warning through the global tsunami warning system to put out to sea where the heights of tsunami waves would be virtually undetectable. We believe that the "100-m wave" reported in the NOAA NGDC Tsunami Catalog for the 1674 "Indonesian Tsunami" is dubious. In support of this belief, we note that this particular event has not been included in other South American tsunami catalogues and reviews provided by Berninghausen (1962), Lomnitz (1970), Soloviev and Go (1975), and Lockridge (1985).

Regional Tsunamis are tsunamis generated by major earthquakes near the coast of Central and South America but relatively far removed from the study region. This includes the main tsunami generation zone off southern Chile. The 1960 Chilean tsunami is the best example of this type of tsunami. Waves from this event caused catastrophic damage on the coasts of Hawaii and Japan, and produced 4 m run-up as far away as the northwestern coast of the Sea of Okhotsk (Russia). Regional tsunamis are a serious threat to the coast of Peru. Depending on the source region, ships docked at the Peru and northern Chile harbour facilities could have tsunami warning times of an hour or so after the recording of the main earthquake shock to move into deeper offshore waters.

Local Tsunamis are those generated by major earthquakes in close proximity to the coasts of Peru and northern Chile. In the past, there have been several catastrophic earthquakes in this region, notably the major events of 1586, 1604, 1724, 1746, 1835, 1868, and 1877, when generated tsunami waves with reported wave heights from 16 up to 24–26 m. Since wave arrival times would be less than an hour, ships docked at the corresponding facilities typically would not have sufficient warning to avert the waves. Clearly, *local tsunamis* are a major threat to cause damage within the study region.

The possibility of catastrophic *Landslide-generated tsunamis* has received little attention for the coast of South America. There have been several cases where relatively small earthquakes (known as "tsunami earthquakes") have been accompanied by significant tsunamis. For example the 1960 Peruvian earthquake with magnitude $M = 6.9$ produced a tsunami run-up of 9 m (Abe, 1979; Pelayo and Wiens, 1990, 1992). Another spectacular example is the tsunamigenic earthquake of 1978 with $M = 5.6$. One of the possible reasons for these unusually strong tsunamis (compared to the magnitudes of the earthquakes) is that these earthquakes could trigger massive submarine landslides on the continental slope of Peru and Chile. A recent example is the catastrophic 1998 Papua New Guinea earthquake during which 2,200 people were killed by tsunami waves generated by a local landslide triggered by the earthquake (González, 1999; Satake and Tanioka, 2003). This type of combined source (earthquake + landslide) may be responsible for a number of unusual tsunamis. Destructive tsunamigenic landslides may also occur in the absence of earthquakes, as in the case of the 1994 Skagway tsunami, Alaska (Kulikov *et al.*, 1996). Von Huene *et al.* (1989) found curved scarps cutting the middle slope of the continental margin of northern Peru marking a slip-surface block measuring 20 km $\times$ 33 km, which was displaced downslope; the authors indicate that if the slip occurred suddenly, a local 50 m-high tsunami would have been generated. The possibility of landslide-generated tsunamis for the coast of Peru needs to be examined.

3. Subduction Zones of South America and General Seismicity

The high mountain peaks and volcanoes of the Andes, along with the great earthquakes along the coast of South America, are dramatic manifestations of ocean–continent plate convergence (Norabuena *et al.*, 1998). Western South America is the only major subduction zone where an entire oceanic slab descends under a continent. Here, the oceanic Nazca Plate subducts beneath the South American continent. The interaction of these two gigantic plates is the main reason for very high seismic activity in this region (Figure 1), some of the highest in the world. Several studies have been devoted to determining the exact subduction geometry of this zone (cf. Kelleher, 1972; Schneider and Sacks, 1987; Beck and Ruff, 1989; Lindo *et al.*, 1992). The contact zone between oceanic and continental plates is typically a zone of high seismic activity. With the exception of Japan, the Pacific continental border of South America has the highest seismic activity in the world (Lomnitz, 1970). Major earthquakes with magnitudes greater than 8.0 occur every 5–10 years in this region.

The study of South American earthquakes has a long history. Barazangi and Isacks (1976) undertook a careful examination of about 6,000 events. Detailed statistics on earthquakes can be found in Askew and Algermissen (1985) and Silgado (1985). The distribution of earthquake hypocenters clearly indicates that the Nazca Plate is subducting at an inclination of

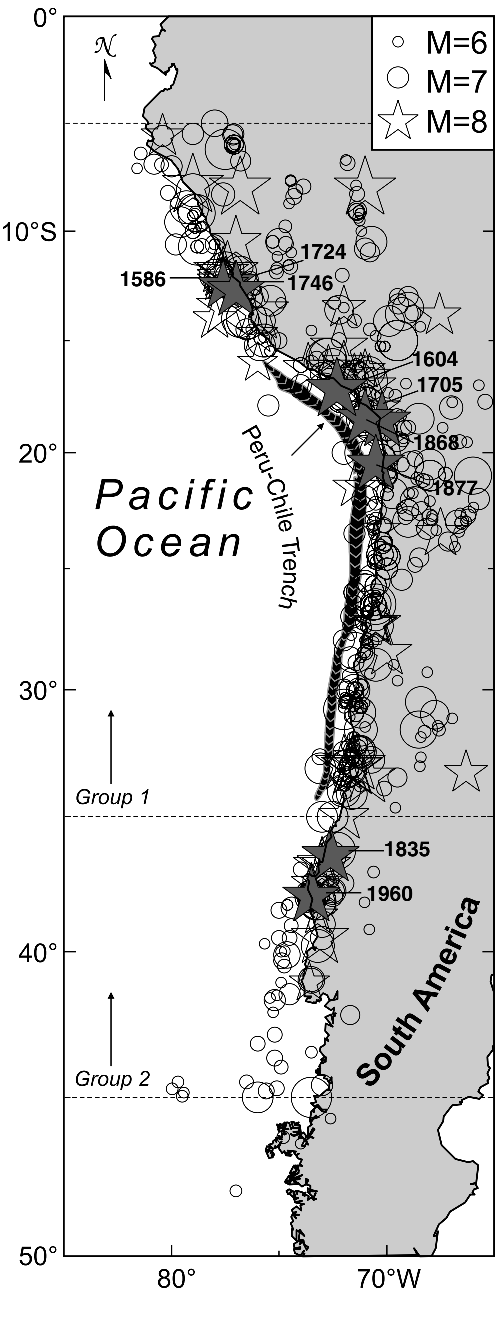

Figure 1. Epicenters of tsunamigenic earthquake sources for the entire observational period (1471–2003) for the coasts of Chile and Peru between 5 and 45° S.

45–60°, so at 100 km from the trench the depth of earthquake hypocenters are 100–200 km. Such deep-focused earthquakes are unlikely to produce tsunami waves, explaining why the epicenters of most of the known tsunamigenic earthquakes are located close to the coastline. As emphasized by Lomnitz (1970), the epicenters of tsunamigenic earthquakes are situated between the axes of Peru–Chilean Trench and the mainland coast. This is also the zone of the strongest earthquakes (Figure 1).

Kelleher (1972) examined rupture zones of large South American earthquakes and attempted to forecast likely locations of future earthquakes using a "*seismic gap theory*". By mapping the rupture zones of large earthquakes ($M \geq 7.7$), he identified segments of the shallow seismic zones that have not ruptured in many decades (Figure 2). Following seismic gap theory, gaps between rupture zones tend to be the focus of large-magnitude earthquakes. One of the zones detected by Kelleher (1972) as an area of strong future earthquakes is a segment along the Peru Trench located between the rupture zones of the 1940 and 1942 earthquakes (12–14° S). Two years after publication of Kelleher's 1972 paper, a large tsunamigenic earthquake with $M_w = 8.0$ occurred in this exact area (Figure 2). The 1996 Chimbote earthquake ($M_w = 7.5$) occurred in a seismic gap subduction-zone located between 8 and 10° S (the first strong Peruvian earthquake since the 17th century). There are controversial opinions about the physical background and efficiency of seismic gap forecasts (cf. Kagan and Jackson, 1991; Nischenko and Sykes,1993; Rong *et al.*, 2003 and the Nature debate at http://www.nature.com/nature/debate/earthquake/). However, for the area of Peru and northern Chile the Kelleher's forecast was found to be quite precise (cf. Dewey and Spence, 1979; Beck and Ruff, 1989).

In light of Kelleher's prediction, the extensive seismic gap between 15 and 24° S assumes significant importance (cf. Lockridge, 1985). In the past, several strong tsunamigenic earthquakes occurred in this area, including the 1604 First Arica Earthquake with a magnitude 8.5 at 17° S, a large earthquake in 1705 at 18.6° S, the Second (Great) Arica Earthquake of 1868 with a magnitude 8.5, and the 1877 Tarapaca Earthquake at 19.6° S with a magnitude of 8.3 (the respective epicenters are indicated by stars in Figure 2). Tsunami heights associated with the earthquakes of 1604, 1705, 1868, and 1877 were 16, 8, 16, and 24 m respectively. Thus, even by crude estimates, tsunamis with *wave heights of about 16 m will occur in this region once every 100 years*. In March 2001, Rabinovich *et al.* (2001) wrote: *"The region between 15 and 24° S, straddling the Peru/Chile border, lays a "seismic gap" which has not experienced an earthquake since 1877. Thus, it has high potential for a major earthquake of magnitude greater than 8.0… Tsunamis with wave heights of about 16 m … are likely to occur in the near future"*.

Three months after the Rabinovich *et al.* (2001) prediction, on June 23, 2001, a catastrophic earthquake ($M_w = 8.4$) occurred off the coast of

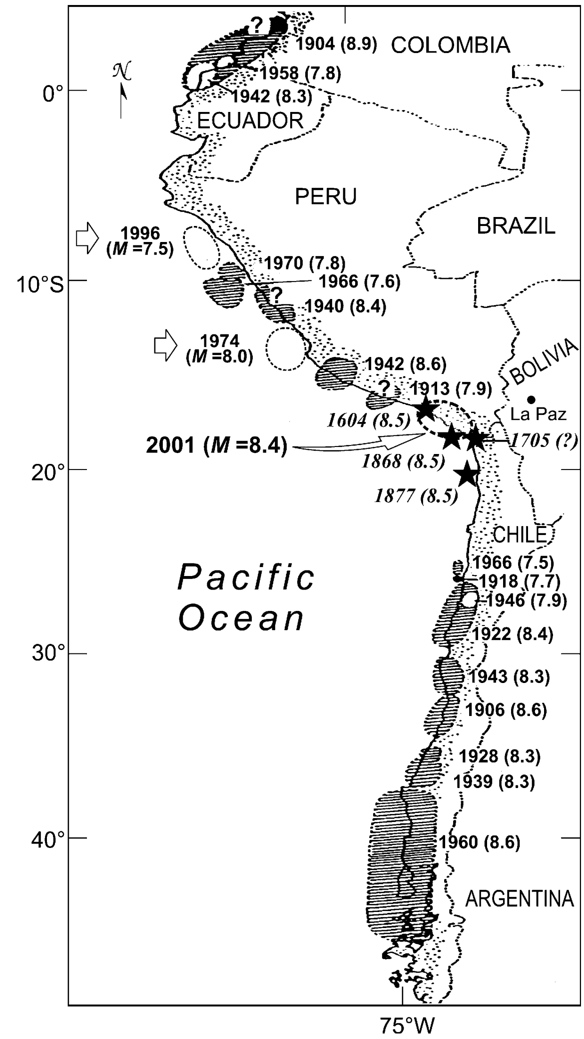

Figure 2. Rupture zones (hatched areas) of large magnitude ($M \geq 7.5$) earthquakes for the west coast of South America during the 20th century (from Kelleher, 1972). The 1974 earthquake occurred in the seismic gap between the 1940 and 1942 rupture zones, located northward from the 1974 rupture zone; the 1996 earthquake occurred in the 8–10° S gap. The 2001 Southern Peru Earthquake occurred in the extensive seismic gap between 15 and 24° S coinciding with the region of historical earthquakes in 1604, 1705, 1868, and 1877 (the epicenters of these four earthquakes are indicated by stars).

southern Peru in the expected seismic gap region (Figure 2). The source of the earthquake was located 175 km west of Arequipa (Peru) and about 600 km southeast of Lima (Tavera *et al.*, 2002; Rodriguez-Marek and Edwards, 2003). A tsunami generated by this earthquake was recorded around the entire rim of the Pacific Ocean (cf. Goring, 2002; Rabinovich and Stephenson, 2004) and claimed at least 23 lives. The maximum tsunami run-up estimated by the International Tsunami Survey Team in the Camaná–Chala area (southern Peru) was more than 9 m (Okal *et al.*, 2002).

4. Earthquake Recurrence

We have used the catalogue data for South America from Askew and Algermissen (1985), Silgado (1985), Gusiakov (2003) and the NOAA/NESDIS/National Geophysical Data Center to examine spatial and temporal distributions for the epicenters of South American earthquakes. First, we determined the epicenters of all known earthquakes with magnitudes $M \geq 6.0$ (Group 2) in the area bounded by 5–45° S and 65–85° W (Figure 1). This box includes epicenters of ''local'' and ''regional'' earthquakes in Peru and Chile. We also determined the epicenters in a smaller box defined by 5–35° S and 65–85° W containing only ''local'' earthquakes (Group 1).

The temporal distribution of earthquakes in Group 1 (Figure 3a) has an irregular structure, with many more earthquakes in 20th century than in earlier centuries. This is related to improvements in seismological observations rather than to higher seismic activity. The historical data on earthquake magnitudes are mainly based on chronicles and descriptions of damage, aftershocks and the observed seismic intensity during the events. Naturally, these data exist only for strong events. That is why there is no information about earthquakes with $M \leq 7.0$ occurring in this region before the second half of 19th century. For this reason, we constructed a separate plot for earthquakes occurring during the past 103 years (Figure 3b). Using these data, we estimated the probability distributions and recurrence times (return periods) for earthquakes with different magnitudes. However, as mentioned above, deep-focused inland earthquakes, even those with large epicenter areas, cannot generate tsunamis. Lockridge (1985) constructed a plot of the epicenters for tsunamigenic earthquakes in Peru and northern Chile for the period 1586–1974 and found that the epicenters of all known earthquakes – except for two dubious cases (both from 1928) – occurred in the narrow zone between the Peru–Chile Trench and the 80-km wide coastal zone. These results are in good agreement with the recent results by Gusiakov (2003). Based on Lockridge's and Gusiakov's findings, we selected tsunamigenic earthquakes (i.e., earthquakes having the potential to generate tsunamis).

We used data from various earthquake catalogues but found that the catalogue by Gusiakov (2003) is the most complete. In particular, the total number of tsunamigenic events of Group 1 with $M \geq 6.0$ in his catalogue is 323 (including 70 occurring before 1900), while the NOAA/NEDIS

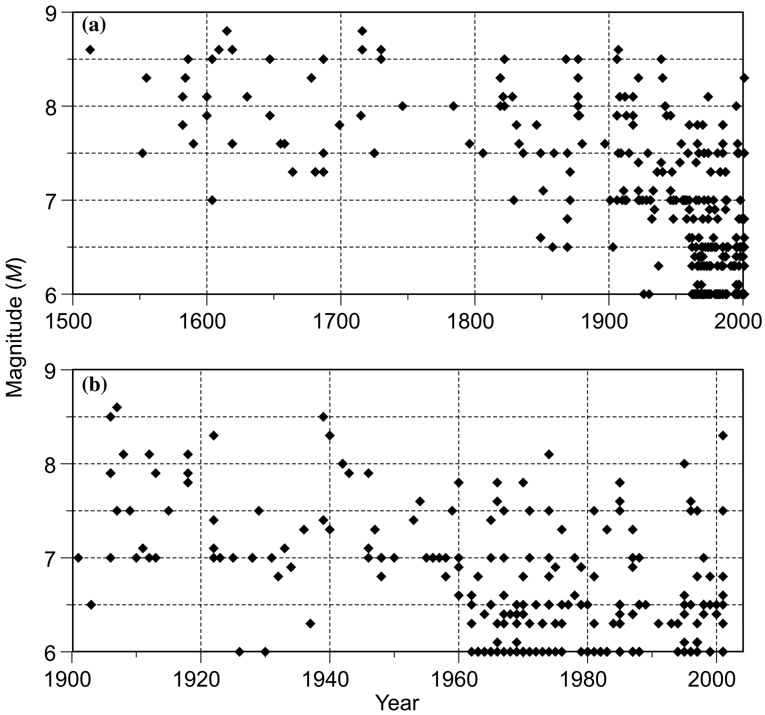

Figure 3. Dates of earthquakes in Peru and northern Chile with magnitudes $M \geq 6.0$ for the periods (a) 1500–2003 and (b) 1901–2003.

Catalogue contains information on 145 (48) events. As a consequence, the following analysis is mainly based on Gusiakov's database.

Using all available data covering the period from 1471 (the first event in this region chronicled by Gusiakov, 2003) to 2003, we determined the frequency of occurrence distribution of earthquakes as a function of magnitude (Table I). We then used these distributions to construct plots of earthquake recurrence (return periods). For comparison, we examined two cases: one that encompasses all data and another that uses only tsunamigenic earthquakes (with epicenters located in the ocean and coastal zone). Results show that there are fewer earthquakes in the second group and their corresponding return periods are much longer (Table II and Figure 4). However, for extreme events (M > 8.4–8.5) the predictions for both groups coincide, indicating that all major earthquakes occurring in this region may be considered as "tsunamigenic".

For tsunamigenic earthquakes with magnitude value M_j , we counted the total number of events (N_j) with $M \geq M_j$ and then estimated the respective value of recurrence period T_e^j as $T_e^j = T_0/N_j$, where T_0 spans the full observational period (Figure 4). Recurrence period plots have been

Table I. Estimated parameters for Gumbel's asymptotic tsunamigenic earthquake distributions for the region of Peru and southern Chile.

Observational period (years)	Number of events (N)	Mean period (years) ($\bar{T}$)	First distribution		Third distribution		
			α	β	M_{∞}	μ	k
1471–2003	323	1.65	104.1	0.77	9.1	3.1	2.0
1901–2003	253	0.40	895.5	1.15	9.1	6.2	3.0

Table II. Computed tsunamigenic earthquake magnitudes (M) for different return periods.

Observational period	Return period (years)						
	2	5	10	20	50	100	200
1471–2003	6.30	7.45	8.00	8.34	8.62	8.76	8.86
1901–2003	7.30	7.83	8.10	8.31	8.52	8.64	8.73
1749–1974 (Silgado)	–	–	–	–	8.04	8.35	8.47

constructed for the entire historical period 1471–2003 (Figure 4a) and for the last 100 years (Figure 4b). Various distributions are used to estimate the return periods of earthquakes as function of magnitude. The cumulative frequency–magnitude distribution follows a power-law relationship, known as ''Guttenberg–Richter relation'' (Pacheco *et al.*, 1992; Kagan, 1999). Weichert (1980) used well-defined variable observation periods for each magnitude range; however we could not define such completeness periods, and therefore applied in our study the theory of *Extreme Statistics* (Gumbel, 1962) to determine earthquake return periods for earthquakes with various magnitudes (M). According *to Gumbel's First asymptotic distribution*, the probability, $F(M)$, of an earthquake event with magnitude less than M may be presented as

$$F(M) = \exp\left(-\alpha e^{-\beta M}\right), \tag{1}$$

where α and β are positive empirical parameters. The return periods, T_e, may be estimated as

$$T_e(M) = \frac{\bar{T}}{[1 - F(M)]}, \tag{2}$$

where $\bar{T} = T_0/N$ is the mean recurrence period of an event (earthquake) with $M \geq 6.0$ and N is the total number of events. Note that $1 - F(M)$ is the probability of an earthquake event with magnitude larger than or equal to M. The asymptotic relation for large M, $1 - F(M) \cong \alpha e^{-\beta M}$, yields a simple expression for M and T_e:

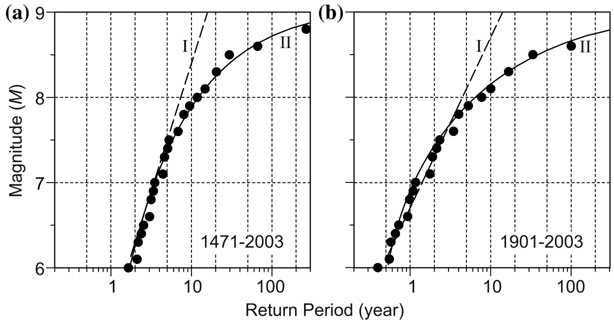

Figure 4. Return periods of tsunamigenic earthquakes in Peru and northern Chile having magnitudes $M \geq 6.0$ for the periods (a) 1471–2003 and (b) 1901–2003. Numerals (I) and (II) denote Gumbel's first and third asymptotic distributions.

$$M = a\log(T_e) + b, \tag{3}$$

where $a = (\beta \log e)^{-1} = 2.30\beta^{-1}$ and $b = a\log(\alpha/\bar{T})$ Figure 4 uses a log scale for T_e, so M in expression (3) is a straight line. A standard least-squares procedure was applied to calculate parameters a and b. Results yield the following regression expressions:

$$M = 3.0\log(T_e) + 5.40 \quad \text{for } 1471 - 2003, \tag{4a}$$

$$M = 2.0\log(T_e) + 6.70 \quad \text{for } 1901 - 2003, \tag{4b}$$

Parameters α and β were then estimated as $\alpha = \overline{T} \cdot 10^{b/a}$ and $\beta = (a\log e)^{-1} = 2.30a^{-1}$. Findings are summarized in Table I.

Although the first asymptotic distribution (1) and the respective empirical relations (4a) and (4b) accurately describe the recurrence of moderate earthquakes (with $M \leq 7.5$), they fail for large earthquakes (with $M > 7.5$) (Figure 4). The main reason is the existence of a natural limit for earthquake magnitudes, $M = M_\infty$. The extreme statistics of such processes are best described by the *Gumbel's Third asymptotic distribution* (also called the '*Cauchy distribution*') (Gumbel, 1962):

$$F(M) = \exp\left[-\left(\frac{M_\infty - M}{M_\infty - \mu}\right)^k\right], \tag{5}$$

where M_∞, μ and k are empirical parameters. It follows from (5) and (2) that

$$M = M_\infty - (M_\infty - \mu)[-\ln(1 - \bar{T}/T)]^{1/k}. \tag{6}$$

Taking into account the general seismicity in South America and the statistics of earthquakes in the region, we assigned $M_\infty = 9.1$ and calculated the other parameters from the distribution of $M_j(T_e^j)$ (see Table I).

Finally, using expressions (4a,b) for earthquakes with $M \leq 7.5$ and expression (6) for $M > 7.5$, we have estimated values of M for various return periods (Table II). For comparison, we also include the results by Silgado (1978) who used data available at that time for the period 1749–1974 to estimate the recurrence of major earthquakes in study region.

As indicated by Figure 3, earthquake data prior to 1900 are scarce and unreliable, especially for relatively weak earthquakes. As a result of improved earthquake statistics for the 20th century, there is a significant increase in all estimated values for $M < 8.2$ compared with the pre-1900 data. Due to the absence of information on earthquakes with $M \leq 7.0$ before the middle of the 19th century, the M-line defined by (4a) (Figure 4a) is much steeper than the M-line for the 20th century defined by (4b) (Figure 4b). That is why return periods (T_e) based on the 1471–2003 statistics for weak earthquakes are significantly longer than those based only on the 1901–2003 data. However, for strong earthquakes $(M > 8.0)$ the two distributions look similar. The slightly greater magnitudes (for $T_e > 20$ years) for the 1471–2003 distribution, compared with the 1901–2003 and the Silgado 1749–1974 estimated magnitudes, can be attributed to contributions of the $M = 8.8$ earthquakes of 1615 and 1716 which affected the return-period statistics. We further note that the pre-1900 (i.e., pre-instrumental) magnitude values are not necessarily reliable.

5. Tsunami Heights from Earthquake Magnitudes

Computed values of M for different T_e (1901–2003 statistics) were used to estimate tsunami run-up heights through the application of three different methods (Table III). The first method uses the well-known relation of Iida (cf. Murty, 1977):

$$m = 2.61M - 18.44, \tag{7}$$

where $m = \log_2(h)$ is the *tsunami magnitude* and h is the tsunami run-up height (in meters) on the coast in the vicinity of the tsunami source. The second method, recently proposed by Abe (1995), has the form:

$$\log(h) = 0.5M - 3.30. \tag{8}$$

A problem with these methods, however, is that they present integral relations between earthquake magnitudes and tsunami wave heights and do not take into account local peculiarities of a given region, such as local topographic amplification of arriving tsunami waves. For the region of Peru and Chile, Silgado (1978) used earthquake and tsunami statistics for the period 1749–1974, to derive the more regional relation:

$$\log(h) = 0.79M - 5.70. \tag{9}$$

Table III. Tsunami wave heights (in meters) for different return periods estimated from earthquake magnitudes.

Authors	Return period (years)						
	2	5	10	20	50	100	200
Iida	1.5	3.8	6.5	9.5	13.9	17.3	20.4
Abe	2.2	4.1	5.6	7.2	9.1	10.5	11.6
Silgado	1.2	3.1	5.0	7.3	10.7	13.4	15.7

Results from all three models are listed in Table III. These models agree well for return periods of 5–20 years but indicate significant difference for larger periods. For example, for $T_e = 200$ years, Iida's formula (7) gives 20.4 m while Abe's formula (8) gives only 11.6 m. The main reason for this discrepancy is the insufficient accuracy of the seismically derived estimates of maximum tsunami wave heights presented in Table III.

Figure 5 shows a scatter plot of earthquakes and tsunamis (69 events spanning the period 1575–2001) for the region of Peru and northern Chile. The correlation between earthquake and tsunami magnitudes is $r^2 \approx 0.48$. According to Figure 5, an earthquake with magnitude $M = 8.5$ can generate a tsunami with magnitude as high as $m = 4.5$ or as low as $m \sim 0$. The respective empirical relationships are:

$$m = (0.80 \pm 0.20)M - (4.32 \pm 1.40), \tag{10a}$$

$$\log(h) = (0.24 \pm 0.06)M - (1.30 \pm 0.42). \tag{10b}$$

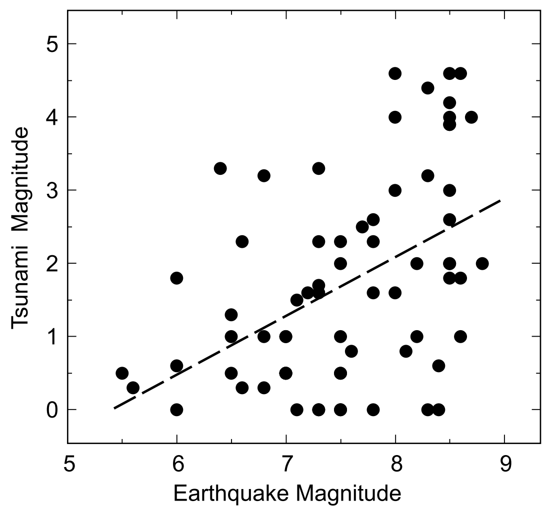

Figure 5. Relationship between earthquake magnitudes (M) and tsunami magnitudes (m) for the coasts of Peru and northern Chile.

For a return period of 200 years, the relationships (10) give a wave height of 6.3 m. However, if we take into account the confidence intervals and increase the first coefficient in expression (10a) from 0.80 to 1.00, we obtain for this return period a tsunami wave height of 21.3 m (very close to Iida's), while for a coefficient of 0.60, we obtain a wave height of only 1.1 m. This factor of 20 difference emphasizes the inaccuracy of seismological estimates of expected tsunami heights. We should also take into account that models (7)–(10) present *average* empirical relationships between earthquake magnitudes and tsunami wave heights and are apparently not appropriate for estimating *maximum* tsunami wave heights (cf. Figure 5).

6. Estimates of Tsunami Heights from Tsunami Data

The seismological relationships for estimating tsunami height, presented in the previous section, likely provide the only method for obtaining approximate values of expected tsunami heights for regions with poor tsunami statistics. However, for the coasts of Peru and Chile there are almost 500 years of observational data on tsunami run-up (cf. World Data Center for Solid Earth Geophysics (WDC-CEG), Boulder, CO, and Gusiakov, 2003). This enables us to apply the Extreme Statistics theory (Gumbel, 1962) directly for tsunami heights and to estimate tsunami risk for this region based on these data. Two types of database search were conducted: "Tsunami Event" and "Tsunami Run-up". Both search modes were used to select all data for the Pacific coast of South America from 5 to 35° S, including Peru and northern Chile.

From the "Tsunami Event" search, we selected 71 events for the period 1562–2003.[1] From the "Tsunami Run-up" search mode, we found more than 450 run-up values for various coastal sites. Instrumental recording of sea level variations became systematic only in the 20th century, so that the quality of modern and historical data is markedly different. In effect, we have statistics for "small" tsunami events (wave heights less than 1–2 m) only for the last 90 years.

Figure 6 shows the spatial distribution of historical tsunami run-up along the coasts of Peru and northern Chile. Despite the irregular distribution of reporting sites along the coast, the tsunami risk for the entire coast seems to be *quasi-uniform* in that it does not appear to depend on latitude. This can be explained by the almost uniform spatial distribution of tsunami sources

[1]For both earthquakes and tsunamis, we tried to use *all available statistics* instead of trying to cover the same time periods for the earthquake and tsunami series. Consequently, results for earthquakes span the period 1471–2003 while those for tsunamis span the period 1562–2003.

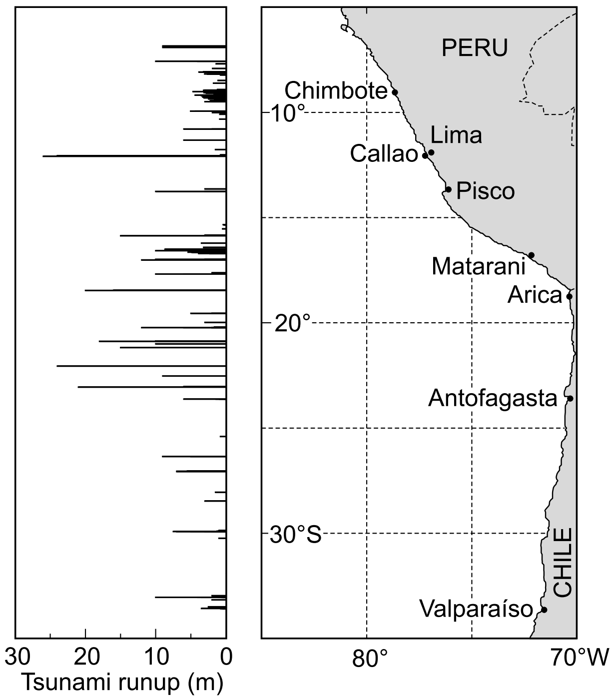

Figure 6. Distribution of tsunami run-up heights along the coasts of Peru and northern Chile for the period 1562–2003.

(earthquake epicenters) (Figure 1) and the relatively smooth and uniform structure of the coastline and continental shelf seafloor topography along the coast of Peru and Chile. Only in the northern part of the region (close to the Ecuador coast) is there a diminishing risk of tsunamis, presumably related to the coastal shielding of tsunami waves originating in the south. Naturally, run-up heights cannot be expected to be uniformly distributed along the coast for a *single* tsunami event. Maximum run-up heights are normally observed near the source, as evident from Figure 7 for the 1868, 1877, 1966, and 2001 tsunamis. Statistically, tsunami heights decrease away from the source region according to $R^{-1/2}$, where R is the distance from the source. However, for purposes of this analysis, the statistical distribution of tsunami run-up heights for all events is treated as uniform from 5 to 35° S latitude.

In reality, the spatial distribution of tsunami heights along the coast may be significantly modified by local topography, coastal irregularities, shelf resonance effects, and other topographical factors (see, for example, Figure 3 in Bourgeois *et al.*, 1999 or Figure 1 in Okal *et al.*, 2002). Thus, to correctly estimate tsunami risk for a selected site (i.e., to provide '*local tsunami-zoning*', cf. Go *et al.*, 1985) the above effects need to be examined for a large segment

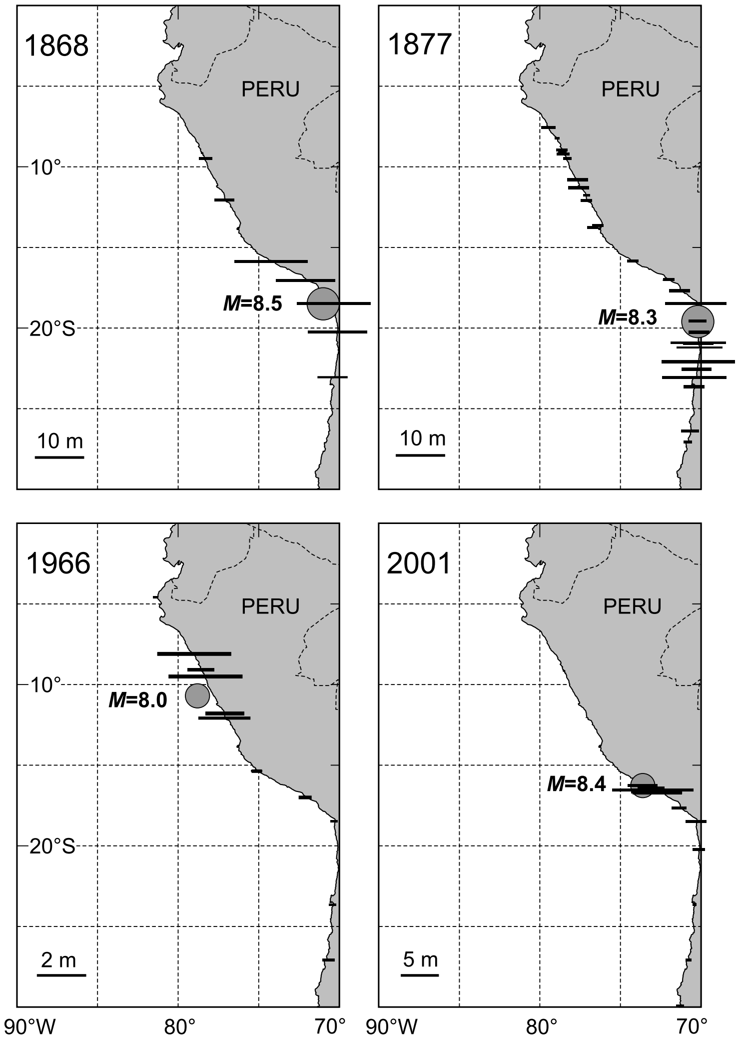

Figure 7. Distribution of tsunami run-up heights along the coasts of Peru and northern Chile for: (a) the 1868 Second Arica Earthquake with $M = 8.5$; (b) the 1877 Tarapaca earthquake with $M = 8.3$; (c) the 1966 Peru earthquake with $M = 8.0$; and (d) the 2001 Southern Peru earthquake with $M = 8.4$.

of the neighboring coasts. A combination of careful examination of the coastal observational data and numerical modeling of tsunami propagation and transformation along the coast would significantly improve the quality and reliability of any data-based analysis (cf. Khramushin and Shevchenko, 1994; Mofjeld *et al.*, 1999). In the present work, we neglect possible resonant features of selected sites and estimate the general tsunami risk for the region as a whole.

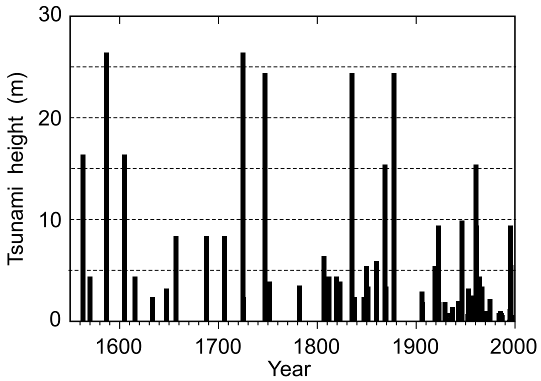

Figure 8. Dates of historical tsunami events for the coast of Peru from 1562 to 2003.

Figure 8 is a stick plot of tsunami run-up recorded in the Peru region from 1562 to 2003. This plot shows that in historical past there were at least five events with tsunami run-up heights of 24 m or more (1586, 1724, 1746, 1835, and 1877) and several other events with wave heights more than 15 m. The time series appears to be strongly stochastic with stationary variability. For this reason, we use statistical analysis of extremes originally developed for river flood events. Hazen (1930) was probably the first to suggest using the logarithmic normal probability distribution (cf. Gumbel, 1962) to describe the recurrence of extreme events, in particular, flood flows. This approach was found to be efficient in estimating return periods for tsunamis of different height. The probability density for this distribution has the form

$$f(h) = \frac{1}{h\sigma\sqrt{2\pi}} \exp\left(-\frac{\ln^2(h/\beta)}{2\sigma^2}\right), \tag{11}$$

where h is the tsunami run-up, β is the median of the distribution, and σ is the root mean square (RMS) of $\ln(h/\beta)$. The probability $F(h)$ of an event less than h is

$$F(h) = \int_{-\infty}^{h} f(h)dx \tag{12}$$

and, therefore,

$$F(h) = \frac{1}{\sqrt{2\pi}} \int_{-\infty}^{s} e^{-(s^2/2)} ds, \qquad s = \frac{\ln(h/\beta)}{\sigma}. \tag{13}$$

Table IV. Estimated parameters for lognormal distribution of tsunami heights for the coasts of Peru and southern Chile.

Observational period (T_0)	Number of events (N)	Mean return period (years) ($\bar{T}$)	Median of distribution (m) (β)	RMS of ln(h/β) (σ)
1562–2003	71	6.22	1.71	1.67
1901–2003	43	2.40	0.74	1.53

We have estimated parameters β and σ for the entire historical period (1562–2003) and for the last 100 years (1901–2003). The results are summarized in Table IV.

Taking into account (2) and using parameters from Table IV, we have estimated return periods, T_t, for different tsunami run-up heights (Table V). In Figure 9 we use a lognormal scale to present the tsunami height probability distribution; the straight line in this format denotes the log-normal distribution approximation. According to this figure, the historical data from 1562 to 1900 are devoid of small tsunamis with run-up heights less than 1 m. In the 20th century, coinciding with the beginning of sea level surveys and instrumental recording, the number of relatively frequent small tsunamis increases dramatically, similar to the number of earthquakes with $M < 7.0$ (compare with Figure 4). For this reason, for small heights (less than 2–3 m), the distribution for the entire data set falls below the distribution for recent data. However, for large run-up (larger than 3–4 m) the graphs converge.

The event corresponding to a 50-year recurrence period is about 15 m while the tsunami run-up corresponding to a 100-year return event is 25 m. The latter value appears to be statistically reliable, taking into account the five historical events with $h \geq 24$ m (Figure 8). A value of 40 m for the 200-year period may be considered too high (during the entire observational period of about 500 years there were no reliable events with recorded run-ups more than 27–28 m). However, we need to take into account the incompleteness of the historical record: as was mentioned above, the first post-tsunami field survey in Peru's history was provided only after the 1996 Chimbote tsunami (Bourgeois *et al.*, 1999). We also note the spectacular

Table V. Computed tsunami run-up heights (m) for different return periods.

Observational period	Return periods, T_t (years)					
	5	10	20	50	100	200
1562–2003	–	1.4	4.9	13.4	24.1	40.0
2001–2003	1.0	2.9	6.3	14.4	25.0	40.0

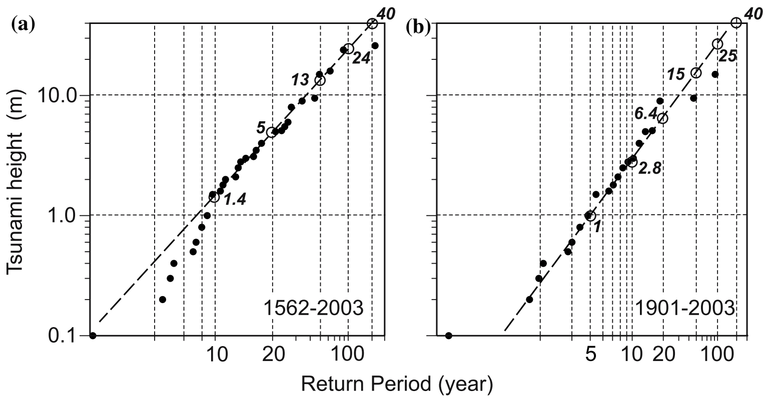

Figure 9. Return periods of tsunami run-up heights calculated for historical tsunami records for the periods 1562–2003 (all data) and 1901–2003 (recent data). Numbers on the graphs denote tsunami wave heights (m).

example of the 1993 Okushiri earthquake with $M = 7.8$ that occurred in the Sea of Japan (a region which is considered as relatively seismically calm compared with the Kamchatka, Kuril, Japan or South American subduction zones). This earthquake generated a catastrophic tsunami wave that struck various parts of Okushiri Island with wave heights typically ranging from 5 to 10 m but then reaching 32 m in a small valley on the southern part of the coast (González, 1999). On this basis, we speculate that 40-m high tsunami waves associated with $M = 8.6$–8.8 earthquakes in the past probably impacted scarcely populated areas of the coasts of Peru and northern Chile. Because of increased population, future events will likely have more devestating consequences.

7. Discussion and Conclusions

We conducted a thorough hazard analysis based on a detailed examination of all known tsunamigenic earthquakes and observed tsunami run-up for the coasts of Peru and northern Chile for zones bounded by 5–35° S latitude. Calculations based on *tsunamigenic earthquake estimates* indicate earthquake magnitudes 8.52, 8.64, and 8.73 corresponding to 50, 100, and 200-year return periods, respectively. Based on three different empirical relations between earthquake magnitudes and tsunamis (including those obtained for the Pacific coast of South America), we estimated expected tsunami wave heights for various return periods. Different methods were found to give quite different results, revealing the highly approximate nature of tsunami estimates based on the seismological approach. Averaging the three different estimates, we get 11.2 m (50 years), 13.7 m (100 years), and 15.9 m (200 years). For comparison, Iida's method (cf. Murty, 1977) gives maximum values of tsunami wave heights of 13.9, 17.3, and 20.4 m respectively. It is noteworthy that both the "averaged" and "maximum" *seismological* estimates of tsunami wave heights for this region are significantly smaller than the actually observed tsunami run-up during the 1586, 1724, 1746, 1835, and 1877 events (more than 24 m). The reason for this disagreement may, in part, be related to incomplete parameterization of earthquake ruptures. However, we cannot exclude also possible influence of *strong resonant effects* at specific sites: the 32-m tsunami runup in "Tsuji valley" (a tiny valley on the southern coast of Okushiri Island) during the 1993 tsunami in the Sea of Japan (González, 1999) clearly demonstrated significant importance of such local resonant effects, which cannot be taken into account by simple seismological relationships (7)–(10).

According to our findings, the best estimates of extreme tsunami wave heights and respective return periods are obtained using observed tsunami data. Fortunately, for the coasts of Peru and northern Chile, there exist almost 500 years of tsunami statistics, including 43 events that occurred during the past century, a time when the quality of the observations has significantly improved. To estimate maximum tsunami heights for different return periods, we used the "Tsunami Event" and "Tsunami Run-up" databases. Preliminary findings from the tsunami wave height data indicate that the "Likely Case" event – corresponding to a 50-year recurrence period for these coasts – is about 15 m. The tsunami run-up corresponding to a 100-year return event – is about 25 m in good agreement with actual observations.

We note that the asymptotic probabilities of extremes for earthquakes and tsunamis are considerably different for large return periods (longer than 10 years). In particular, extreme earthquakes have limited magnitudes whereas extreme tsunami runup has unlimited height (compare Figures 4 and 9). Earthquake magnitude is controlled by subduction zone parameters: each seismically active region has a specific $M = M_\infty$ which cannot be exceeded. A maximum $M_\infty = 9.5$ apparently applies to the Cascadia and southern Chile subduction zones (Roy Hyndman, Personal Communication, 2004), while for Peru and northern Chile the maximum $M_\infty \approx 9.1$. The two factors playing a principal role in limiting earthquake magnitudes are:

(1) *The fault size*. Earthquake magnitude is limited by the maximum fault area. This area is strictly limited by the subduction zone and normally has an elliptical form oriented along the strike of the subduction thrusts. Subduction thrust faults generate earthquakes over a limited depth range: they are aseismic in their seaward updip portions and landward downdip of a critical point (Hyndman *et al.*, 1997). The typical width (w) of seismogenic zones is up to 100 km, maximum 150 km. At the same time the length (l) of these zones are limited by the width: $l/w \leq 2 - 3$ (this means that the epicenter

area cannot be too long), and only for a few exceptional areas (in particular, for Cascadia and southern Chile) $l/w \sim 6$ (Roy Hyndman, personal communication, 2004).

(2) *The critical shear stress*. The higher the accumulated stress on the fault area, the stronger will be the earthquake energy release in the subduction zone. However, this stress cannot be greater than a certain critical value depending on the oceanic crust properties, because the crust breaks, and has a similar value for most great earthquakes.

In contrast to the case for earthquake magnitudes, the asymptotic distribution of tsunami wave heights possesses no upper limit. This then begs the question: Why do earthquake magnitudes have an asymptotic limit, whereas tsunamis, which are related to earthquake magnitude, have unlimited heights? One possible explanation is the inadequate statistics for observed tsunami run-up (which is poorer than for earthquakes). In effect, it is impossible to resolve statistically the discrepancy of the observed maximum values using the lognormal regression line. On the other hand, unlimited distributions of tsunami wave heights are in fact observed for regions with good tsunami statistics (in particular, for Japan) and there is a clear analogy between tsunamis and river floods, which have well established unlimited lognormal distributions (We can even paraphrase the well known epigraph from Gumbel's book: "*However big tsunamis get, there will always be a bigger one coming; so says one theory of extremes, and experience suggests it is true*"). Thus, we can assume that the difference between earthquake and tsunami distributions has a physical, rather than a statistical, cause. In particular:

(1) Earthquakes are a major, but not the only source, of tsunami waves: these waves may be generated by volcano explosions, submarine landslides and even by an asteroid impact.
(2) The nature of tsunami height statistics differs from that for earthquake magnitudes. Bathymetry and coastline irregularities seem to be major factors determining the extreme statistical distribution. Scattering effects cause additional stochastization of tsunami height distribution. The key factor in destructive manifestation of tsunami waves at some sites is the resonant influence of topography. It is impossible to predict how sharp will be the resonance: the 1993 Okushiri tsunami with local 32-m waves, destructive tsunami waves in Port Alberni Inlet during the 1964 Alaska tsunami, and even the 525 m tsunami waves associated with the 1958 Lituya landslide are just a few spectacular examples of resonant influence of local topography (see additional examples in Murty, 1977).

In conclusion, we suggest that attention be given to the region between 15 and 24° S along the Peruvian and southern Chilean coasts. Before 2001, this region constituted a "seismic gap" which had not experienced an earthquake since 1877, despite the fact that there had been catastrophic earthquakes and tsunamis in this region in the past (specifically, 1604, 1705, 1868, and 1877). Thus, the gap region had a high potential for a major earthquake and associated tsunami. Based on the seismic gap theory, Rabinovich *et al.* (2001) had argued that an earthquake of magnitude greater than 8.0 and a tsunami with wave heights up to 16 m was expected for this region. The actual earthquake, which occurred three months later, on June 23, 2001, had magnitude $M = 8.4$ and epicenter at 16.3° S, 73.6° W. This earthquake generated a destructive tsunami with wave height more than 9 m. For this event, the seismic gap theory was remarkably accurate. Taking this concept one step further, we now predict that a strong earthquake and associated tsunami will occur in the vicinity of northern Chile between 19 and 28° S where there have been no strong earthquakes for the past 100 years.

Acknowledgments

This research was partially sponsored by the RFBR project 03-05-64583. The authors would like to thank Garry Rogers, Roy Hyndman, and John Ristau (Pacific Geoscience Center, Sidney, BC) for their help with seismological data, helpful discussion and productive comments. Patricia Kimber helped draft the figures.

References

Abe, K.: 1979, Size of great earthquakes of 1837–1974 inferred from tsunami data, *J. Geophys. Res.* **84**(B4), 1561–1568.

Abe, K.: 1995, Estimate of tsunami run-up heights from earthquake magnitudes, In: Y. Tsuchiya and N. Shuto (eds), *Tsunami: Progress in Prediction, Disaster Prevention and Warning*, Kluwer, Dordrecht, pp. 21–35.

Askew, B. and Algermissen T. (eds): 1985, Catalog of Earthquakes for South America – Hypocenter and Intensity Data, *Earthquake Mitigation Program in the Andean Region*, 7A, CERESIS, Lima, Peru, 190 pp.

Barazangi, M. and Isacks, B. L.: 1976, Spatial distribution of earthquakes and subduction of the Nazca Plate beneath South America, *Geology* **4**(11), 686–692.

Beck, S. L. and Ruff, L. J.: 1989, Great earthquakes and subduction along the Peru Trench, *Phys. Earth Planet Interiors* **57**, 199–224.

Berninghausen, W. H.: 1962, Tsunamis reported from the west coast of South America 1562–1960, *Bull. Seismol. Soc. Am.* **52**(4), 915–921.

Bourgeois, J., Petroff, C., Yeh, H., Titov, V., Synolakis, C., Benson, B., Kuroiwa, J., Lander, J., and Norabuena, E.: 1999, Geologic setting, field survey and modeling of the Chimbote, northern Peru, tsunami of 21 February 1996, *Pure Appl. Geophys.* **154**(3/4), 513–540.

Burroughs, S. M., and Tebbens, S. F.: 2003, Power law scaling and recurrence intervals of tsunamis, *EOS* **84**, Abstract NG31A-0606.

Dewey, J. W., and Spence W.: 1979, Seismic gaps and source zones of recent large earthquakes in coastal Peru, *Pure Appl. Geophys.* **117**, 1148–1171.

Geist, E. I.: 2002, Complex earthquake rupture and local tsunamis, *J. Geophys. Res.* **107**(B5), ESE 2-1 – ESE 2-16, 10.1029/2000JB000139.

Go, Ch. N., Kaistrenko, V. M. and Simonov, K. V.: 1985, A two-parameter scheme for tsunami hazard zoning, *Marine Geodesy* **9**(4), 469–476.

González, F. I.: 1999, Tsunami!, *Sci. Am.* May, 56–65.

Goring, D. G.: 2002, Response of New Zealand waters to the Peru tsunami of 23 June 2001, *N. Z. J. Mar. Freshw. Res.* **36**, 225–232.

Gumbel, E.: 1962, *Statistics of Extremes*, Columbia University Press, New York, 275 pp.

Gusiakov, V. K.: 2003, *Historical Tsunami Data Base for the Pacific,* Version 3.9, CD-ROM, Tsunami Laboratory, ICMMG RAS, Novosibirsk, Russia.

Hazen, A.: 1930, *Flood Flows, A Study of Frequencies and Magnitudes,* Wiley, New York, 183 pp.

Heinrich, P., Gomez, J.-M., Guibourg, S., and Ihmle, P. F.: 1998, Modeling of the February 1996 Peruvian tsunami, *Geophys. Res. Lett.* **25**(14), 2687–2690.

Horikawa, K. and Shuto, N.: 1983, Tsunami disasters and protection measures in Japan, In: K. Iida and T. Iwasaki (eds), *Tsunamis – Their Science and Engineering*, Terra Sci., Tokyo, 9–22.

Hyndman, R. D., Yamano, M., and Oleskevich, D. A.: 1997, The seismogenic zone of subduction thrust faults, *Island Arc.* **6**, 244–260.

Kagan, Y. Y.: 1999, Universality of the seismic–moment frequency relation, *Pure Appl. Geophys.* **155**, 537–573.

Kagan, Y. Y., and Jackson, D. D.: 1991, Seismic gap hypothesis: Ten years after, *J. Geophys. Res.* **96**, 21419–21431.

Kelleher, J. A.: 1972, Rupture zones of large South American earthquakes and some predictions, *J. Geophys. Res.* **77**(11), 2087–2103.

Khramushin, V. N. and Shevchenko, G. V.: 1994, A method of detailed tsunami zoning for coastal Aniva Bay, *Oceanology* **34**(2), 192–197.

Kulikov, E. A., Rabinovich, A. B., Thomson, R. E., and Bornhold, B. D.: 1996, The landslide tsunami of November 3, 1994, Skagway Harbor, Alaska, *J. Geophys. Res.* **101**(C3), 6609–6615.

Lay, T. and Wallace, T. C.: 1995, *Modern Global Seismology*, Intern. Geophys. Series, Vol. 58. Academic Press, San Diego, CA, 521 pp.

Lindo, R., Dorbath, C., Cistenas, A., Dorbath, L., Ocola L., and Morales, M.: 1992, Subduction geometry in central Peru from a microseismicity survey: First results, *Tectonophysics* **205**, 23–29.

Lockridge, P. A.: 1985, *Tsunamis in Peru–Chile*, World Data Center A for Solid Earth Geophysics, Report SE-39, U.S. Department of Commerce, NOAA, Boulder, CO, 97 pp.

Lomnitz, C.: 1970, Major earthquakes and tsunamis in Chile during the period 1535 to 1955, *Geolog. Rundsch.* **59**(3), 938–960.

Mofjeld, H. O., González, F. I., and Newman, J. C.: 1999, Tsunami prediction in U.S. coastal regions, in *Coastal and Estuarine Studies*, Vol. 56, American Geophysical Union, pp. 353–375.

Murty, T. S.: 1977, Seismic sea waves – tsunamis, *Bull. Fish. Res. Board Can.* **198**, 337 pp.

Nishenko, S. P., and Sykes, L. R.: 1993, Comment on 'Seismic gap hypothesis: Ten years after' by Y.Y. Kagan and D.D. Jackson, *J. Geophys. Res.* **98**, 9909–9916.

Norabuena, E., Leffler-Griffin, L., Mao, A., Dixon, T., Stein, S. Sacks, I. S., Ocola, L., and Ellis, M.: 1998, Space geodetic observations of Nazca-South America convergence across the Central Andes, *Science* **279**, 358–362, Okal, E. A., Dengler, L., Araya, S., Borrero, J. C., Gomer, B. M., Koshimura, S., Laos, G., Olese, D., Ortiz, M., Swensson, M., Titov, V. V., and Vegas, F.: 2002, Field survey of the Camaná, Peru tsunami of June 23, 2001, *Seism. Res. Lett.* **73**(6), 907–920.

Pacheko, J. F., Scholz, C. H., and Sykes, L. R.: 1992, Changes in frequency-size relationship from small to large earthquakes, *Nature* **355**, 71–73.

Pelayo, A. M. and Wiens, D. A.: 1990, The November 20, 1960 Peru tsunami earthquake: Source mechanism of a slow event, *Geophys. Res. Lett.* **17**(6), 661–664.

Pelayo, A. M. and Wiens, D. A.: 1992, Tsunami earthquakes: slow thrust-faulting events in the accretionary wedge, *J. Geophys. Res.* **97**(B11), 15321–15337.

Planning for Risk: 1988, *Comprehensive Planning for Tsunami Hazard Areas*, Prepared by Urban Regional Research for the National Science Foundation, 246 pp.

Rabinovich, A. B., Shevchenko, G. V., and Sokolova, S. E.: 1992. An estimation of extreme sea levels in the northern part of the Sea of Japan, *La mer* **30**, 179–190,

Rabinovich, A. B., Kulikov, E. A., and Thomson R. E.: 2001, Tsunami risk estimation for the coasts Peru and Northern Chile. *International Tsunami Symposium 2001*, Seattle, WA, Proceedings, CD, pp. 281–291.

Rabinovich, A. B. and Stephenson, F. E.: 2004, Longwave measurements for the coast of British Columbia and improvements to the tsunami warning capability, *Nat. Hazards* **32**(3), 313–343.

Rodriguez-Marek and Edwards, C. (eds): 2003, Southern Peru Earthquake of 23 June 2001. Reconnaissance Report, *Earthquake Spectra*, **19**(Suppl.)

Rong, Y., Jackson, D. D. and Kagan, Y. Y.: 2003, Seismic gaps and earthquakes, *J. Geophys. Res.* **108** (BIO) (ESE 6-1 – 6-1, 2471, doi:10.1029/2002JB002334).

Satake, K. and Tanioka, Y.: 2003, The July 1998 Papua New Guinea earthquake: Mechanism and quantification of unusual tsunami generation. *Pure Appl. Geophys.* **160**, 2087–2118.

Schneider, J. F., and Sacks, I. S.: 1987, Stress in the contorted Nazca Plate beneath Southern Peru from local earthquakes, *J. Geophys. Res.* 92(B13), 13877–13902.

Silgado, E.: 1978, Recurrence of tsunamis in the western coast of South America, *Marine Geodesy* **1**(4), 347–354.

Silgado, E.: 1985, *Destructive Earthquakes of South America 1530–1894*, Earthquake Mitigation Program in the Andean Region, Vol. 10, CERESIS, Lima, Peru, 328 pp.

Soloviev, S. L. and Go, Ch. N.: 1975, *Catalogue of Tsunamis on the Eastern Shore of the Pacific Ocean*, Nauka Publ. House, Moscow, 204 pp. (in Russian; English translation: Canadian Transl. Fish. Aquatic Sci., No. 5078, Ottawa, 293 pp., 1984).

Synolakis, C. E. and Skjelbreia, J. E.: 1993, Evolution of maximum amplitude of solitary waves on plane beaches, *J. Waterw. Port Coastal Ocean Eng.* ASCE, **119**, 323–342.

Tavera, H., Buffon, E., Bernal, I., Antayhua, Y., and Vilcapoma, L.: 2002, The Arequipa (Peru) earthquake of June 23, 2001, *J. Seismol.* **6**, 279–283.

Von Huene, R., Bourgeois, J., Miller, J., and Pautot, G.: 1989, A large tsunamogenic landslide and debris flow along the Peru Trench, *J. Geophys. Res.* **94**(B2), 1703–1714.

Weichert, D. H.: 1980, Estimation of the earthquake recurrence parameters for unequal observation periods for different magnitudes, *Bull. Seism. Soc. Am.* **70**(4), 1337–1346.